PERGAMON

International Journal of Heat and Mass Transfer 45 (2002) 3559–3569

International Journal of HEAT and MASS TRANSFER

www.elsevier.com/locate/ijhmt

Improvement in performance on laminar counterflow concentric circular heat exchangers with external refluxes

Chii-Dong Ho *, Ho-Ming Yeh, Wen-Yi Yang

Department of Chemical Engineering, Tamkang University, Tamsui, Taipei 251, Taiwan, ROC

Received 3 August 2001; received in revised form 6 February 2002

Abstract

Considerable improvement of heat transfer in laminar counterflow concentric heat exchangers is obtainable by inserting in parallel an impermeable, resistless sheet to divide an open duct into two subchannels for double-pass operations with external refluxes. Efficiency improvement in heat transfer has been investigated analytically by using an orthogonal expansion technique. The results of improvement in heat transfer efficiency are represented graphically and compared with those in a single-pass operation. The influences of improvement-sheet location and reflux ratio on the enhancement of transfer efficiency as well as on the increment of power consumption have been discussed.

1. Introduction

The study of laminar forced convection heat and mass transfer in a conduit with neglecting the effect of axial conduction is known as the Graetz problem [1,2]. Dealing with multistream or multiphase problems coupling through conjugated conduction–convection conditions at the boundaries is called conjugated Graetz problems [3–9]. Applications of the recycle-effect concept in the design and operation of the equipment with external or internal refluxes can effectively enhance the effect on heat and mass transfer, leading to improved performance in separation processes and reactor designs, such as loop reactors [10,11], air-lift reactors [12,13] and draft-tube bubble columns [14,15].

The purposes of the present study are to investigate the improvement of performance and to develop an orthogonal expansion technique [16–24] to the heat transfer in concentric heat exchangers with external refluxes. The solutions to these problems are obtained by using the method of separation of variables, where the resulting eigenvalue problem is solved by the orthogonality conditions. This work includes the influence of recycling on heat transfer and the improvement of transfer efficiency with reflux ratio and Graetz number as parameters.

2. Theoretical formulations

2.1. Temperature distributions in concentric tubes of double-pass devices with recycle

Consider the heat transfer in concentric tubes with length L, inside diameter $2R$ of the outer tube, an impermeable sheet with negligible thickness δ ($\ll 2R$) and thermal resistance is inserted as the inner tube with inside diameter of $2\kappa R$. Before entering the inner tube for a double-pass operation as shown in Fig. 1(a), the fluid with volume flow rate V and the inlet temperature T_i will mix with the fluid exiting from the outer tube with the volume flow rate MV and the outlet temperature T_F, which is regulated by using a conventional pump. The fluid is completely mixed at the inlet and outlet of the tube.

The following assumptions are made in the present analysis: constant physical properties and wall temperatures of the outer tubes; purely fully developed laminar

* Corresponding author. Tel.: +886-2-26266632; fax: +886-2-26209887.

E-mail address: cdho@mail.tku.edu.tw (C.-D. Ho).

0017-9310/02/$ - see front matter
PII: S0017-9310(02)00072-8

Nomenclature

C_p	heat capacity, J/kg k
D	hydraulic radius, m
d_{mn}	coefficient in the eigenfunction $F_{a,m}$
e_{mn}	coefficient in the eigenfunction $F_{b,m}$
F_m	eigenfunction associated with eigenvalue λ_m
f	friction factor
g_c	conversion factor, kg m/s^2 N
Gz	Graetz number, $4V/\alpha\pi L$
G_m	function defined during the use of orthogonal expansion method
$\overline{h}$	average heat transfer coefficient, kW/m^2 K
h_{fs}	friction loss in conduit, m^2/s^2
I_h	improvement of heat transfer, defined by Eq. (45)
I_p	increment of power consumption, defined by Eq. (51)
k	thermal conductivity of the fluid, kW/m K
L	conduit length, m
M	reflux ratio, reverse volume flow rate divided by input volume flow rate
$\overline{Nu}$	Nusselt number
P_0	hydraulic dissipated energy
R	inside diameter of the outer tube, m
Re	Reynolds number
S_m	expansion coefficient associated with eigenvalue λ_m
T	temperature of fluid, K
V	input volume flow rate of conduit, m^3/s
v	velocity distribution of fluid, m/s
$\overline{v}$	average velocity of fluid, m/s
r	radial coordinate, m
z	axial coordinate, m

Greek symbols

α	thermal diffusivity of fluid, m^2/s
δ	thickness of the impermeable sheet, m
ξ	longitudinal coordinate, z/L
η	transversal coordinate, r/R
θ	dimensionless temperature, $(T-T_i)/(T_w-T_i)$
κ	ratio of channel thickness
λ_m	eigenvalue
μ	viscosity of fluid, kg/ms
ρ	density of the fluid, kg/m^3
ψ	dimensionless temperature, $(T-T_w)/(T_i-T_w)$

Subscripts

a	in forward flow channel
b	in backward flow channel
F	at the outlet of a double-pass device
i	at the inlet
L	at the outlet, $\xi = 1$
0	in a single-pass device without recycle
w	at the wall surface

flow on the entire length in each subchannel; negligible end effect, axial conduction and thermal resistance of inner tubes. After the following dimensionless variables are introduced:

$$\eta = \frac{r}{R}, \quad \xi = \frac{z}{L}, \quad \psi_a = \frac{T_a - T_w}{T_i - T_w},$$
$$\psi_b = \frac{T_b - T_w}{T_i - T_w}, \quad \theta_a = 1 - \psi_a = \frac{T_a - T_i}{T_w - T_i},$$
$$\theta_b = 1 - \psi_b = \frac{T_b - T_i}{T_w - T_i}, \quad Gz = \frac{4V}{\alpha\pi L}. \tag{1}$$

The velocity distributions and equations of energy in dimensionless form may be obtained as

$$\frac{v_a(\eta)R^2}{\alpha L}\frac{\partial\psi_a(\eta,\xi)}{\partial\xi} = \frac{1}{\eta}\left[\frac{\partial}{\partial\eta}\left(\eta\frac{\partial\psi_a(\eta,\xi)}{\partial\eta}\right)\right], \tag{2}$$

$$\frac{v_b(\eta)R^2}{\alpha L}\frac{\partial\psi_b(\eta,\xi)}{\partial\xi} = \frac{1}{\eta}\left[\frac{\partial}{\partial\eta}\left(\eta\frac{\partial\psi_b(\eta,\xi)}{\partial\eta}\right)\right], \tag{3}$$

$$v_a(\eta) = 2\overline{v_a}\left(1 - \left(\frac{\eta}{\kappa}\right)^2\right), \quad 0 \leqq \eta \leqq \kappa, \tag{4}$$

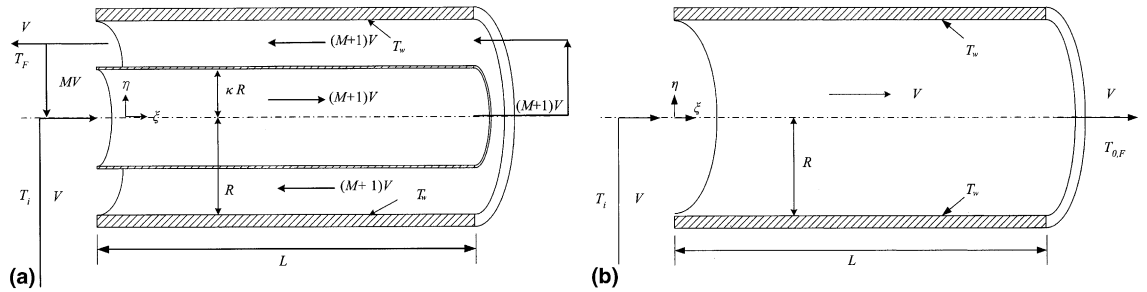

Fig. 1. Double- and single-pass concentric circular heat exchangers.

$$v_b(\eta)=\left\{2\overline{v_b}\Big/\left[\frac{1-\kappa^4}{1-\kappa^2}-\frac{1-\kappa^2}{\ln\frac{1}{\kappa}}\right]\right\}\times\left[1-\eta^2+\left(\frac{1-\kappa^2}{\ln 1\kappa}\right)\ln\eta\right],\quad \kappa\leqq\eta\leqq 1, \tag{5}$$

in which

$$\overline{v_a}=\frac{(M+1)V}{\pi(\kappa R)^2}\quad\text{and}\quad \overline{v_b}=-\frac{(M+1)V}{\pi R^2-\pi(\kappa R)^2}.$$

The boundary conditions for solving Eqs. (2) and (3) are

$$\frac{\partial\psi_a(0,\xi)}{\partial\eta}=0, \tag{6}$$

$$\psi_b(1,\xi)=0, \tag{7}$$

$$\frac{\partial\psi_a(\kappa,\xi)}{\partial\eta}=\frac{\partial\psi_b(\kappa,\xi)}{\partial\eta}, \tag{8}$$

$$\psi_a(\kappa,\xi)=\psi_b(\kappa,\xi) \tag{9}$$

and the dimensionless outlet temperature is

$$\theta_F=1-\psi_F=\frac{T_F-T_{\rm i}}{T_{\rm w}-T_{\rm i}}. \tag{10}$$

Inspection of Eqs. (2), (3) and (6)–(9) shows that the inlet conditions for both subchannels are not specified a priori and reverse flow occurs. The analytical solutions to both flow patterns may be obtained by the use of an orthogonal expansion technique with the eigenfunction expanding in terms of an extended power series.

Separation of variables in the form

$$\psi_a(\eta,\xi)=\sum_{m=0}^{\infty}S_{a,m}F_{a,m}(\eta)G_m(\xi), \tag{11}$$

$$\psi_b(\eta,\xi)=\sum_{m=0}^{\infty}S_{b,m}F_{b,m}(\eta)G_m(\xi) \tag{12}$$

applied to Eqs. (2) and (3) leads to

$$G_m(\xi)=\mathrm{e}^{-\lambda_m(1-\xi)} \tag{13}$$

$$F''_{a,m}(\eta)+\frac{F'_{a,m}(\eta)}{\eta}-\frac{v_a(\eta)R^2\lambda_m}{\alpha L}F_{a,m}(\eta)=0, \tag{14}$$

$$F''_{b,m}(\eta)+\frac{F'_{b,m}(\eta)}{\eta}-\frac{v_b(\eta)R^2\lambda_m}{\alpha L}F_{b,m}(\eta)=0 \tag{15}$$

and also the boundary conditions in Eqs. (6)–(9) can be rewritten as

$$F'_{a,m}(0)=0, \tag{16}$$

$$F_{b,m}(1)=0, \tag{17}$$

$$S_{a,m}F'_{a,m}(\kappa)=S_{b,m}F'_{b,m}(\kappa), \tag{18}$$

$$S_{a,m}F_{a,m}(\kappa)=S_{b,m}F_{b,m}(\kappa) \tag{19}$$

combination of Eqs. (18) and (19) yields

$$\frac{F'_{a,m}(\kappa)}{F_{a,m}(\kappa)}=\frac{F'_{b,m}(\kappa)}{F_{b,m}(\kappa)} \tag{20}$$

in which the eigenfunctions $F_{a,m}(\eta)$ and $F_{b,m}(\eta)$ were assumed to be polynomials to avoid the loss of generality. With the use of Eqs. (16) and (17), we have

$$F_{a,m}(\eta)=\sum_{n=0}^{\infty}d_{mn}\eta^n,\quad d_{m1}=0,\quad d_{m0}=1\quad\text{(selected)}, \tag{21}$$

$$F_{b,m}(\eta)=\sum_{n=0}^{\infty}e_{mn}\eta^n,\quad d_{m1}=0,\quad d_{m0}=1\quad\text{(selected)}. \tag{22}$$

Substituting Eqs. (21) and (22) into Eqs. (14) and (15), all the coefficients d_{mn} and e_{mn} may be expressed in terms of eigenvalues λ_m by using Eqs. (16) and (17), as referred to in Appendix A. Therefore, it is easy to solve all eigenvalues from Eq. (20) and the eigenfunctions associated with the corresponding eigenvalues are also well defined by Eqs. (21) and (22). These eigenvalues, λ_m, include the sets of positive and negative, each of which is required to satisfy the inlet conditions at both end of the counterflow problem.

It is easy to find the orthogonality conditions as follows:

$$\int_0^{\kappa}\left[\frac{v_a\cdot R^2}{L\cdot\alpha}\right]S_{a,m}S_{a,n}\eta F_{a,m}F_{a,n}\,\mathrm{d}\eta+\int_{\kappa}^{1}\left[\frac{v_b\cdot R^2}{L\cdot\alpha}\right]S_{b,m}S_{b,n}\eta F_{b,m}F_{b,n}\,\mathrm{d}\eta=0, \tag{23}$$

when $n\neq m$. Since

$$\psi_L=\sum_{m=0}^{\infty}S_{a,m}F_{a,m}(\eta)=\sum_{m=0}^{\infty}S_{b,m}F_{b,m}(\eta). \tag{24}$$

From the orthogonality conditions, the general expressions for the expansion coefficients may be achieved. Accordingly, we have

$$\int_0^{\kappa}\psi_L\left[\frac{v_a\cdot R^2}{L\cdot\alpha}\right]S_{a,m}\eta F_{a,m}\,\mathrm{d}\eta+\int_{\kappa}^{1}\psi_L\left[\frac{v_b\cdot R^2}{L\cdot\alpha}\right]S_{b,m}\eta F_{b,m}\,\mathrm{d}\eta=\int_0^{\kappa}\left[\frac{v_a\cdot R^2}{L\cdot\alpha}\right]S_{a,m}^2\eta F_{a,m}^2\,\mathrm{d}\eta+\int_{\kappa}^{1}\left[\frac{v_b\cdot R^2}{L\cdot\alpha}\right]S_{b,m}^2\eta F_{b,m}^2\,\mathrm{d}\eta. \tag{25}$$

Using Eqs. (14) and (15), Eq. (25) can be rewritten as

$$\psi_L\left[\frac{S_{a,m}}{\lambda_m}\kappa F'_{a,m}(\kappa)+\frac{S_{b,m}}{\lambda_m}\left(F'_{b,m}(1)-\kappa F'_{a,m}(\kappa)\right)\right]=S_{a,m}^2\left[\kappa F_{a,m}(\kappa)\frac{\partial F'_{a,m}(\kappa)}{\partial\lambda_m}-F'_{a,m}(\kappa)\frac{\partial F_{a,m}(\kappa)}{\partial\lambda_m}\right]-S_{b,m}^2\left[\kappa F_{a,m}(\kappa)\frac{\partial F'_{a,m}(\kappa)}{\partial\lambda_m}-F'_{a,m}(\kappa)\frac{\partial F_{a,m}(\kappa)}{\partial\lambda_m}\right]. \tag{26}$$

Also, the dimensionless outlet temperature at $\xi = 1$ may be calculated as follows:

$$\begin{aligned}\psi_L &= \frac{\int_0^{\kappa} v_a 2\pi R^2 \eta \psi_a(\eta,1)\,\mathrm{d}\eta}{V(M+1)} \\ &= \frac{2\pi\alpha L}{V(M+1)} \sum \frac{S_{a,m}}{\lambda_m} \left(\int_0^{\kappa} \left(F''_{a,m}\eta + F'_{a,m} \right) \mathrm{d}\eta \right) \\ &= \frac{8}{Gz(M+1)} \sum \frac{S_{a,m}}{\lambda_m} \cdot \kappa \cdot F'_{a,m}(\kappa) \\ &= -\frac{\int_{\kappa}^{1} v_b 2\pi R^2 \eta \psi_b(\eta,1)\,\mathrm{d}\eta}{V(M+1)} \\ &= -\frac{2\pi\alpha L}{V(M+1)} \sum \frac{S_{b,m}}{\lambda_m} \left(\int_{\kappa}^{1} \left(F''_{b,m}\eta + F'_{b,m} \right) \mathrm{d}\eta \right) \\ &= -\frac{8}{Gz(M+1)} \sum \frac{S_{b,m}}{\lambda_m} \cdot \left[F'_{b,m}(1) - \kappa \cdot F'_{b,m}(\kappa) \right]. \end{aligned} \tag{27}$$

Accordingly, once all the eigenvalues have been found, the possible associated expansion coefficients, $S_{a,m}$ and $S_{b,m}$, can be calculated from Eqs. (18), (19), (26) and (27) with ψ_L as an intermediate variable during the calculation procedure. Therefore, the dimensionless outlet temperature ψ_F which is referred to as the bulk temperature, may be calculated by

$$\begin{aligned}\psi_F &= -\frac{\int_{\kappa}^{1} v_b 2\pi R^2 \eta \psi_b(\eta,0)\,\mathrm{d}\eta}{V(M+1)} \\ &= -\frac{2\pi\alpha L}{V(M+1)} \sum \frac{\mathrm{e}^{-\lambda_m} S_{b,m}}{\lambda_m} \left(\int_{\kappa}^{1} \left(F''_{b,m}\eta + F'_{b,m} \right) \mathrm{d}\eta \right) \\ &= -\frac{8}{Gz(M+1)} \sum \frac{\mathrm{e}^{-\lambda_m} S_{b,m}}{\lambda_m} \left[F'_{b,m}(1) - \kappa \cdot F'_{b,m}(\kappa) \right] \end{aligned} \tag{28}$$

and may be examined by Eq. (29) which is readily obtained from the following overall energy balance on outer tube:

$$\begin{aligned}\theta_F = 1 - \psi_F &= \int_0^1 \frac{\alpha 2\pi L}{V} \left(-\frac{\partial \psi_{b,m}(1,\xi)}{\partial \eta} \right) \mathrm{d}\xi \\ &= \frac{8\lambda_m}{Gz} \sum_{m=0}^{\infty} S_{b,m} F'_{b,m}(1) \left(1 - \mathrm{e}^{-\lambda_m}\right). \end{aligned} \tag{29}$$

In Eq. (29) the left-hand side refers to the net outlet energy while the right-hand side is the total amount of heat transfer from outer hot wall to the fluid. After the coefficients, $S_{a,m}$ and $S_{b,m}$ are obtained, the mixed inlet temperature is calculated as follows:

$$\begin{aligned}\psi_a(\eta,0) &= \frac{-(M/(M+1)) \int_{\kappa}^{1} v_b 2\pi R^2 \eta \psi_b(\eta,0)\,\mathrm{d}\eta + V}{V(M+1)} \\ &= -\frac{M}{M+1} \frac{2\pi\alpha L}{V(M+1)} \sum \frac{\mathrm{e}^{-\lambda_m} S_{b,m}}{\lambda_m} \\ &\quad \times \left(\int_{\kappa}^{1} \left(F''_{b,m}\eta + F'_{b,m} \right) \mathrm{d}\eta \right) + \frac{1}{M+1} \\ &= \frac{1}{M+1} \left\{ -\frac{8M}{Gz(M+1)} \sum \frac{\mathrm{e}^{-\lambda_m} S_{b,m}}{\lambda_m} \right. \\ &\quad \left. \times \left[F'_{b,m}(1) - \kappa \cdot F'_{b,m}(\kappa) \right] + 1 \right\}. \end{aligned} \tag{30}$$

Mathematically, with known Graetz number (Gz) and reflux ratio (M), as well as the ratio of channel thickness (κ), the eigenvalues ($\lambda_1, \lambda_2, \ldots, \lambda_m, \ldots$) can be calculated from Eq. (20). Fortunately, it is seen from Eqs. (A.4) and (A.5) in Appendix A that Gz and λ_m always appear together and one may further define a modified eigenvalue as $\lambda^*_m = Gz\lambda_m = \text{constant}$. In this case λ^*_m is independent of Gz and one needs not repeat the computation of λ_m for different Gz.

2.2. Temperature distributions in the single-pass device

For the single-flow device of the same size without recycle the impermeable sheet in Fig. 1(a) is removed, as shown in Fig. 1(b) and thus, $\kappa = 1$. The velocity distribution and equation of energy in dimensionless form may be written as

$$\frac{v_0(\eta)R^2}{\alpha L} \frac{\partial \psi_0(\eta,\xi)}{\partial \xi} = \frac{1}{\eta} \left[\frac{\partial}{\partial \eta} \left(\eta \frac{\partial \psi_0(\eta,\xi)}{\partial \eta} \right) \right], \tag{31}$$

$$v_0(\eta) = 2\overline{v_0}\left(1 - \eta^2\right), \quad 0 \leqq \eta \leqq 1, \tag{32}$$

$$\begin{aligned}&\eta = \frac{r}{R}, \quad \xi = \frac{z}{L}, \quad \psi_0 = \frac{T_0 - T_{\mathrm{w}}}{T_{\mathrm{i}} - T_{\mathrm{w}}}, \\ &\theta_0 = 1 - \psi_a = \frac{T_0 - T_{\mathrm{i}}}{T_{\mathrm{w}} - T_{\mathrm{i}}}, \quad G_Z = \frac{4V}{\alpha\pi L}, \quad \overline{v_0} = \frac{V}{\pi(\kappa R)^2}. \end{aligned} \tag{33}$$

The boundary conditions for solving Eq. (31) are

$$\frac{\partial \psi_0(0,\xi)}{\partial \eta} = 0, \tag{34}$$

$$\psi_0(1,\xi) = 0, \tag{35}$$

$$\psi_0(\eta_0,0) = 1. \tag{36}$$

The calculation procedure for a single-pass device is rather simpler than that for a double-pass device. The dimensionless outlet temperature for single-pass devices ($\theta_{0,F}$) was also obtained in terms of Graetz number (Gz), eigenvalues ($\lambda_{0,m}$), expansion coefficients ($S_{0,m}$) and eigenfunctions ($F_{0,m}(\eta_0)$). The result is

$$\begin{aligned}\psi_{0,F} &= \frac{2\pi\alpha L}{V} \sum \frac{S_{0,m}}{\lambda_m} \left(\int_0^1 \left(F''_{0,m}\eta + F'_{0,m} \right) \mathrm{d}\eta \right) \\ &= \frac{8}{Gz} \sum \frac{S_{0,m}}{\lambda_m} \cdot 1 \cdot F'_{0,m}(1) \end{aligned} \tag{37}$$

and may be examined by Eq. (38), which is readily obtained from the following overall energy balance on the outer tube:

$$\theta_{0,F} = 1 - \psi_{0,F} = \int_0^1 \frac{\alpha 2\pi L}{V}\left(-\frac{\partial\psi_{0,m}(1,\xi)}{\partial\eta}\right)\mathrm{d}\xi = \frac{8\lambda_{0,m}}{Gz}\sum_{m=0}^{\infty} S_{0,m}F'_{0,m}(1)\left(1-\mathrm{e}^{-\lambda_m}\right). \tag{38}$$

3. Improvement of transfer efficiency

The Nusselt number for a double-pass operation with recycle may be defined as

$$\overline{Nu} = \frac{\overline{h}(2R)}{k} = \frac{\overline{h}D}{k} \tag{39}$$

in which the average heat transfer coefficient is defined as

$$q = \overline{h}(2\pi RL)(T_\mathrm{w} - T_\mathrm{i}). \tag{40}$$

Since

$$\overline{h}(2\pi RL)(T_\mathrm{w} - T_\mathrm{i}) = V\rho C_\mathrm{p}(T_F - T_\mathrm{i}) \tag{41}$$

or

$$\overline{h} = \frac{V\rho C_\mathrm{p}(T_F - T_\mathrm{i})}{2\pi RL(T_\mathrm{w} - T_\mathrm{i})} = \frac{V\rho C_\mathrm{p}}{2\pi RL}(1-\psi_F) \tag{42}$$

thus

$$\overline{Nu} = \frac{V}{2\pi\alpha L}(1-\psi_F) = \frac{1}{4}Gz(1-\psi_F) = \frac{1}{4}Gz\theta_F. \tag{43}$$

Similarly, for a single-pass operation without recycle

$$\overline{Nu_0} = \frac{V}{2\pi\alpha L}(1-\psi_{0,F}) = \frac{1}{4}Gz(1-\psi_{0,F}) = \frac{1}{4}Gz\theta_{0,F}. \tag{44}$$

The improvement of performance by employing a double-pass operation with recycle is best illustrated by calculating the percentage increase in heat transfer rate, based on the heat transfer of a single-pass operation with same device dimension and operating conditions, but without impermeable sheet and recycle, as

$$I_\mathrm{h} = \frac{\overline{Nu} - \overline{Nu_0}}{\overline{Nu_0}} = \frac{\psi_{0,F} - \psi_F}{1-\psi_{0,F}} = \frac{\theta_F - \theta_{0,F}}{\theta_{0,F}}. \tag{45}$$

4. Increment of power consumption

4.1. Power consumption in the single-pass device

The friction loss in conduits may be estimated by

$$h_\mathrm{fs} = 4f\cdot\frac{L}{D}\cdot\frac{\overline{v}^2}{2g_\mathrm{c}} \tag{46}$$

where $\overline{v}$ and D denote the bulk velocity in the conduit and the diameters of the conduit, respectively, while f is the friction factor which is the function of Reynolds number, Re. The friction loss in the conduit of a single-pass device is calculated by $P_0 = V\rho h_{\mathrm{fs},0}$.

Table 1
The increment of power consumption with reflux ratio and the ratio of channel thickness as parameters

M	I_p		
	$\kappa = 0.3$	$\kappa = 0.5$	$\kappa = 0.7$
0.5	281	47	57
1.0	502	84	103
3.0	2010	340	414
5.0	4524	767	933

4.2. Increment of power consumption in double-pass devices

For double-pass devices, the average velocity of the fluid and the diameter of conduit are

$$v_0 = \frac{V}{\pi R^2}, \quad v_a = \frac{(M+1)V}{\pi(\kappa R)^2}, \quad v_b = \frac{(M+1)V}{\pi\left(R^2 - (\kappa R)^2\right)}, \tag{47}$$

$$D_0 = 2R, \quad D_a = 2\kappa R, \quad D_b = 2(R - \kappa R) \tag{48}$$

and than we have, for the laminar flow in tube

$$f = \frac{16}{Re} \tag{49}$$

and we have

$$h_\mathrm{fs} \propto \frac{\overline{v}}{D^2}. \tag{50}$$

The increment of power consumption, I_p, may be defined as

$$I_\mathrm{p} = \frac{P - P_0}{P_0} = \frac{V(M+1)\rho(h_{\mathrm{fs},a} + h_{\mathrm{fs},b}) - V\rho h_{\mathrm{fs},0}}{V\rho h_{\mathrm{fs},0}}, \tag{51}$$

where $P = V(M+1)\rho(h_{\mathrm{fs},a} + h_{\mathrm{fs},b})$. Substitution of Eqs. (47) and (48) into Eq. (50) results in Eq. (52) in double-pass devices

$$I_\mathrm{p} = \frac{(M+1)^2}{\kappa^4} + \frac{(M+1)^2}{(1-\kappa^2)(1-\kappa)^2} - 1. \tag{52}$$

Some results for I_p of double-pass devices are presented in Table 1.

5. Results and discussion

The equation of counterflow heat exchangers in concentric circular tubes with uniform outer wall

temperature and with external refluxes has been formulated and solved by the use of the orthogonal expansion technique. Two eigenvalues and their associated expansion coefficients as well as the dimensionless outlet temperatures were calculated for $\kappa = 0.5$, $M = 1$, and $Gz = 1$, 10, 100 and 1000, as shown in Table 2. It was found in Table 2 that due to the rapid convergence, only the first negative eigenvalues is necessary to be considered during the calculation of temperature distributions. The eigenfunctions are expanded in terms of an extended power series as well as $\ln y$ term in the velocity distribution is expanded by Taylor series. As an illustration, comparisons were made to such two series with terms truncated after $n = 25$ and $n = 30$ for an extended power series and $N = 2$ and $N = 3$ for Taylor series. The accuracy of those comparisons was analyzed and some results were represented in Tables 3 and 4 for an extended power series and Taylor series, respectively. It is seen from Tables 3 and 4 that two series agree reasonably well with the terms of $n = 25$ for an extended power series and $N = 2$ for Taylor series, and hence those two series with such selected terms were employed in the calculation procedure in this study.

The application of recycle to heat transfer devices results in two conflicting effect: the desirable preheating effect of the inlet fluid and the undesirable effect of decreasing residence time. The temperature of reflux fluid increases with the residence time, which is inversely

Table 2
Eigenvalues and expansion coefficients as well as dimensionless outlet temperatures in double-pass devices with recycle for $\kappa = 0.5$ and $M = 1$. $Gz\lambda_1 = -35.624$ and $Gz\lambda_2 = -43.387$

Gz	m	λ_m	$S_{a,m}$	$S_{b,m}$	$\psi_F(\lambda_1)$	$\psi_F(\lambda_1, \lambda_2)$
1	1	−35.624	-1.01×10^{-15}	0.00	0.3333	0.3333
	2	−43.387	4.00×10^{-14}	0.00		
10	1	−3.562	-8.58×10^{-2}	4.91×10^{-10}	0.3398	0.3398
	2	−4.339	3.42	0.00		
100	1	−0.356	−3.90	2.23×10^{-8}	0.6253	0.6253
	2	−0.434	1.55×10^{2}	0.00		
1000	1	−0.036	−8.03	4.60×10^{-8}	0.9346	0.9346
	2	−0.043	3.20×10^{2}	0.00		

Table 3
The convergence of power series in Eqs. (21) and (22) with $n = 25$ and 30 with $\kappa = 0.3$ $M = 5$

Gz	n	λ_m	$S_{a,m}$	$S_{b,m}$	ψ_F
1	25	−7.9070	1.70×10^{-3}	-4.58×10^{-6}	0.14359
	30	−7.9212	1.52×10^{-3}	7.99×10^{-5}	0.13078
10	25	−0.7907	3.42	-9.22×10^{-3}	0.23471
	30	−0.7921	3.14	1.64×10^{-1}	0.21563
100	25	−0.0791	2.04×10^{1}	-5.51×10^{-2}	0.68794
	30	−0.0792	1.97×10^{1}	1.03	0.66386
1000	25	−0.0079	3.04×10^{1}	-8.21×10^{-2}	0.95512
	30	−0.0079	3.03×10^{1}	1.59	0.95016

Table 4
The convergence of Taylor series in Eq. (A.3) with $N = 2$ and $N = 3$ ($n = 25$) with $\kappa = 0.7$ and $M = 5$

Gz	N	λ_m	$S_{a,m}$	$S_{b,m}$	ψ_F
1	2	−0.6786	1.49×10^{-1}	6.90×10^{-6}	0.25277
	3	−0.6081	-1.53×10^{-6}	1.76×10^{-6}	0.26782
10	2	−0.0679	7.81×10^{-1}	3.61×10^{-5}	0.71754
	3	−0.0608	-7.28×10^{-6}	8.40×10^{-6}	0.73855
100	2	−0.0068	1.11	5.13×10^{-5}	0.96101
	3	−0.0061	-1.01×10^{-5}	1.03×10^{-5}	0.96490
1000	2	−0.0007	1.16	5.35×10^{-5}	0.99594
	3	−0.0007	-1.02×10^{-5}	1.04×10^{-5}	0.99637

proportional to the inlet volume rate (or the Graetz number) and hence the mixed dimensionless inlet temperature increases with the amount of the reflux fluid (or reflux ratio). Accordingly, it is shown in Figs. 2 and 3 that the dimensionless inlet temperature of fluid after mixing increases with reflux ratio but decrease and increasing Graetz number and with κ going away from 0.5, especially for $\kappa > 0.5$.

At low Graetz number (either small input volume flow rate V or large conduit length L) the residence time is essentially long, the preheating effect by increasing the reflux ratio cannot compensate for the decrease of residence time. However, the recycle-effect has positive influences on heat transfer for the operation of large Graetz numbers, say $Gz > 9$. Comparisons of dimensionless outlet temperatures, θ_F and $\theta_{0,F}$ were made and represented in Figs. 4 and 5. Fig. 4 shows another more practical form of dimensionless outlet temperature θ_F (or $\theta_{0,F}$) vs. Gz with the reflux ratio M as a parameter for $\kappa = 0.5$ while Fig. 5 with the ratio of channel thickness κ s a parameter. It was also found in Figs. 4 and 5 that the dimensionless average outlet temperature decreases with increasing the Graetz number Gz owing to the short

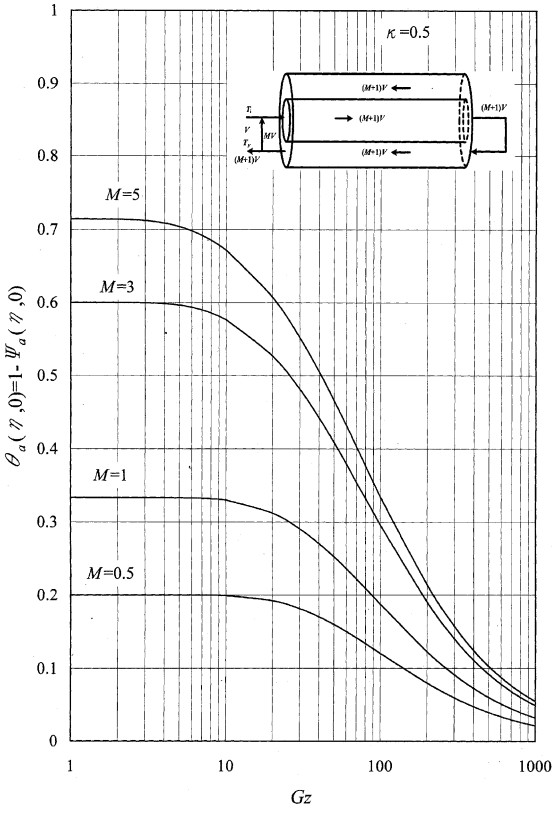

Fig. 2. Dimensionless average inlet temperatures of fluid after mixing. Reflux ratio as a parameter; $\kappa = 0.5$.

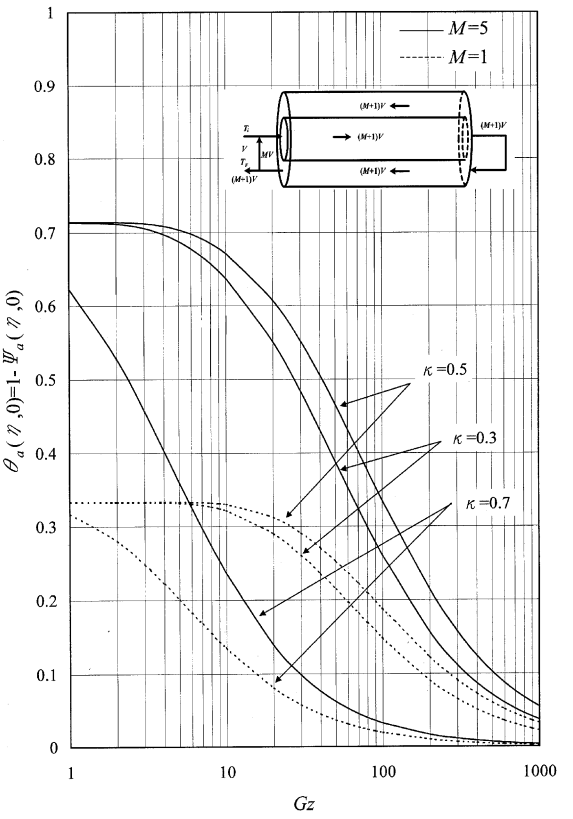

Fig. 3. Dimensionless average inlet temperatures of fluid after mixing. The ratio of channel thickness as a parameter; $M = 1$ and 5.

residence time of fluid, or when the ratio of channel thickness κ goes away from 0.5, especially for $\kappa > 0.5$, but increases as the reflux ratio M increases, due to the preheating effect. The reason why the outlet temperature decreases of $\kappa > 0.5$ is much larger than that of $\kappa < 0.5$ may be considered as that the reduction of heat transfer in inner channel due to increasing the thickness of inner channel with reflux ratio M to decrease the flow velocity can not compensate for the enhancement of heat transfer in outer channel due to decreasing the thickness of outer channel to increase the flow velocity. It is seen from Figs. 4 and 5 that the difference $(\theta_F - \theta_{0,F})$ of outlet temperatures is of minus sign and decreasing with Gz, and then turns to plus sign with any values of M for large Graetz numbers except with $\kappa > 0.5$.

The Nusselt numbers ($\overline{Nu}$ and $\overline{Nu_0}$) and hence the improvement of transfer efficiencies (I_h) are proportional to θ_F (or $\theta_{0,F}$), as shown in Eqs. (43)–(45), so the higher improvement of performance is really obtained by employing a double-pass device, instead of using a single-pass device for large Graetz numbers, if the volumetric flow rate in all devices are kept same. Fig. 6 shows the theoretical average Nusselt numbers $\overline{Nu}$ vs. Gz with the

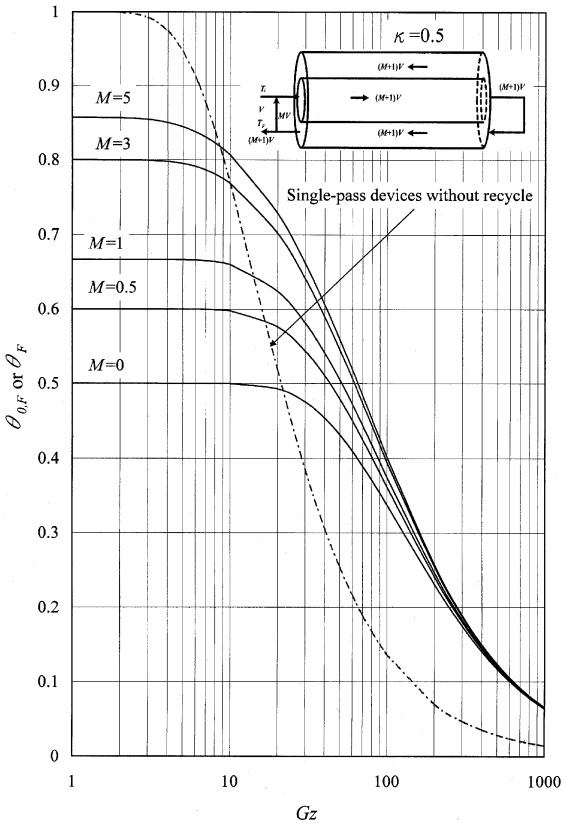

Fig. 4. Dimensionless outlet temperature vs. Gz with reflux ratio as a parameter; $\kappa = 0.5$.

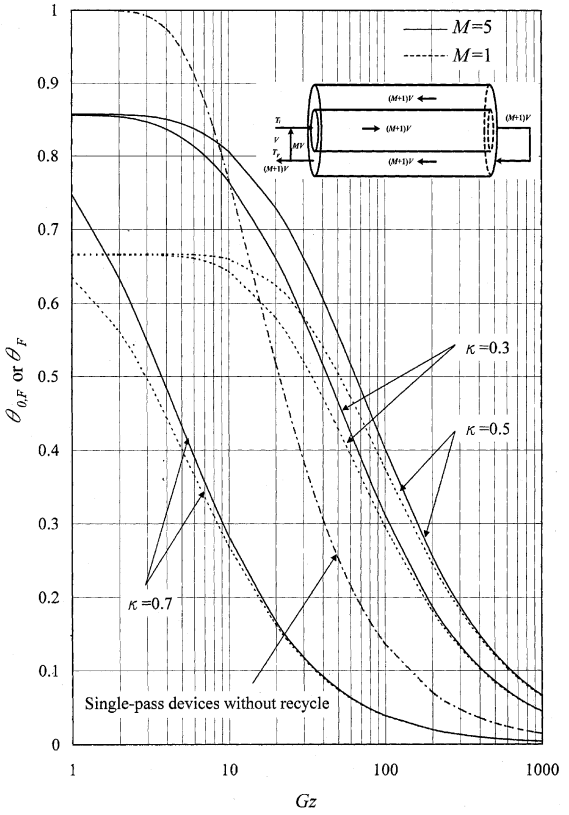

Fig. 5. Dimensionless outlet temperature vs. Gz with κ as a parameter; $M = 1$ and 5.

reflux ratio as a parameter for $\kappa = 0.5$ while Fig. 7 with reflux ratio and the ratio of the channel thickness κ as parameters. On the other hand, as shown in Fig. 6, $(\overline{Nu}_0 - \overline{Nu})$ increases with Gz for intermediate Gz values or with decreasing reflux ratio M, but for $Gz > 20$, $(\overline{Nu} - \overline{Nu}_0)$ then increases with Gz and approaches infinite for large Gz values. It is concluded that Nusselt number increases with M and Graetz number, but decreases with the ratio of channel thickness κ going away from 0.5, especially for $\kappa > 0.5$. Some numerical values of the improvement in performance I_h were given in Table 5. The minus signs in Table 5 indicate that when $Gz = 10$, no improvement in transfer efficiency can be achieved as κ goes away from 0.5 for $M = 3$ and $\kappa > 0.5$ for $M = 5$, and in this case, the single-pass device is preferred to be employed rather than using the four-pass one operating at such conditions. Figs. 6 and 7 demonstrate some results obtained from single-pass and double-pass devices for comparison. With this comparison, the advantage of the double-pass device with external refluxes is evident, especially for large Graetz number. It is found from Figs. 6 and 7 and Table 5 that the improvement of heat transfer efficiency increases with Graetz number as well as reflux ratio, but decreases with κ going away from 0.5, especially for $\kappa > 0.5$.

As an illustration, the power consumption of the single-pass device will be illustrated by the working dimensions as follows: $L = 1.2$ m, $R = 0.2$ m, $V = 1 \times 10^{-4}$ m^3/s, $\mu = 8.94 \times 10^{-4}$ kg/m s, $\rho = 997.08$ kg/m^3. From those numerical values, the friction loss in conduit of a single-pass device was calculated by the appropriate equations and the result is

$$P_0 = V\rho h_{fs,0} = 1.71 \times 10^{-8} \text{ W} = 2.29 \times 10^{-11} \text{ hp}. \quad (53)$$

It is seen from Table 1 that the increment of power consumption does not depend on Graetz number but increases with the reflux ratio or as κ goes away from 0.5, especially for $\kappa < 0.5$. The increment of power consumption between $M = 0.5$ and $M = 1$ is the smallest value as shown in Table 1 while the increment of outlet temperature difference at the same interval is high enough compared to other intervals in Fig. 5. According to head loss increases with respect to reflux ratio, there may exist a suitable selection of operating reflux ratio. The best operating reflux ratio, say the interval between $M = 0.5$ and $M = 1$, would be chosen with the increment of power consumption neglected.

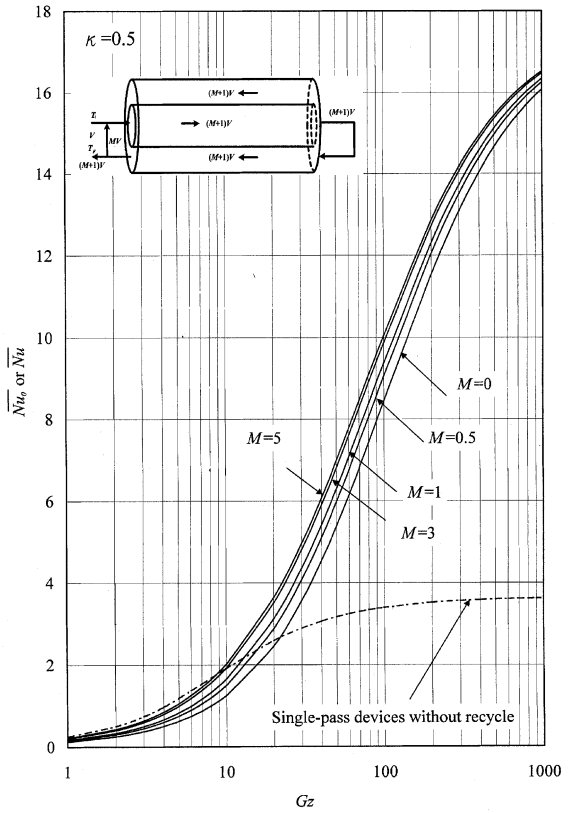

Fig. 6. Average Nusselt number vs. Gz with reflux ratio as a parameter; $\kappa = 0.5$.

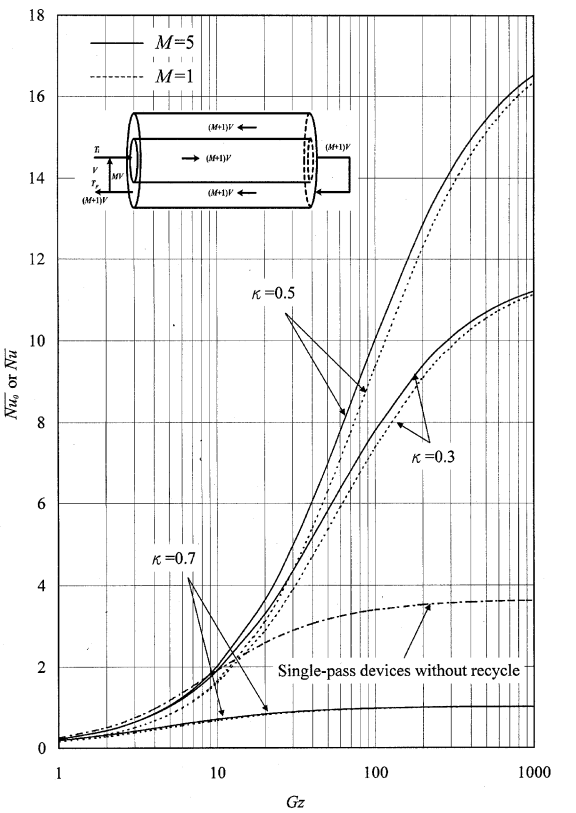

Fig. 7. Average Nusselt number vs. Gz with κ as a parameter; $M = 1$ and 5.

Table 5
The improvement of the transfer efficiency with reflux ratio and the ratio of channel thickness as parameters

I_h (%)	$M = 0$			$M = 1$			$M = 3$			$M = 5$		
	κ			κ			κ			κ		
	0.3	0.5	0.7	0.3	0.5	0.7	0.3	0.5	0.7	0.3	0.5	0.7
$Gz = 1$	−50.1	−50.0	−50.4	−33.4	33.33	−36.51	−20.1	−20.0	−25.27	−14.4	−14.30	−50.29
10	−35.4	−35.0	−67.4	−16.3	−14.07	−64.96	−4.44	0.06	−63.24	0.41	4.97	−67.38
100	100.7	148	−71.8	117.3	175.4	−71.53	126.3	190.2	−71.34	129.3	195.3	−71.81
1000	203.3	343	−72.1	206.8	350.5	−72.09	208.5	355.5	−72.08	209.1	355.5	−72.13

6. Conclusion

Heat transfer through double-pass concentric circular tubes with an impermeable sheet of negligible thermal resistance have been investigated and solved analytically by the use of the orthogonal expansion technique with the eigenfunction expanding in terms of an extended power series. The method for improving the performance in a concentric circular double-pass heat exchanger is presented in this study. Application of the recycle-effect concept in designing a double-pass heat exchanger is technically and economically feasible. Moreover, further improvement in transfer efficiency may be obtained if the channel thickness κ is suitably selected, say $\kappa = 0.5$. The improvement of performance is really obtained by employing double-pass devices, instead of using a single-pass device of same size without recycle, and the improvement increases with increasing the Graetz number and reflux ratio.

It is concluded that the recycle effect can enhance heat transfer for the fluid flowing through a concentric circular heat exchanger under double-pass operations by

inserting an impermeable sheet with negligible thermal resistance. The introduction of reflux has position effects on the heat transfer for large Graetz number and the outlet temperature as well as transfer coefficient increases with increasing reflux ratio. The reason why the improvement decreases with the ratio of channel thickness κ deviating from 0.5, especially for $\kappa > 0.5$ may be considered as that the enhancement of heat transfer in outer channel due to decreasing the thickness of the outer channel to increase the flow velocity cannot compensate for the decrease of heat transfer in the inner channel with reflux ratio M due to driving force in the outer channel is larger than that in the inner channel, leading to reduced performance.

It is apparent that the mathematical treatments developed in this study with concentric circular tubes are only conducted in a heat transfer sense with constant wall temperature, the present theory and method may also be applied to other conjugated Graetz problems in heat- or mass transfer devices with constant heat flux or mass flux on the boundary.

Acknowledgements

The author wishes to thank the National Science Council of the Republic of China for the financial support.

Appendix A

Eqs. (14) and (15) can be rewritten as

$$F''_{a,m}(\eta)+\frac{F'_{a,m}(\eta)}{\eta}-\frac{(M+1)Gz\lambda_m}{2\kappa^2}\left[1-\left(\frac{\eta}{\kappa}\right)^2\right]F_{a,m}(\eta)=0, \tag{A.1}$$

$$F''_{b,m}(\eta)+\frac{F'_{b,m}(\eta)}{\eta}+\frac{(M+1)Gz\lambda_m}{2W_1(1-\kappa^2)} \times\left(1-\eta^2+W_2\cdot\ln\eta\right)F_{b,m}(\eta)=0 \tag{A.2}$$

in which

$$W_1=\left[\frac{1-\kappa^4}{1-\kappa^2}-\frac{1-\kappa^2}{\ln(1/\kappa)}\right],\quad W_2=\left(\frac{1-\kappa^2}{\ln(1/\kappa)}\right)$$

and the term $\ln\eta$ in velocity distributions can be expressed in terms of Taylor series as follows:

$$\ln\eta=(\eta-1)-\frac{(\eta-1)^2}{2}+\frac{(\eta-1)^3}{3}+\cdots+\frac{(\eta-1)^N}{N}. \tag{A.3}$$

Combining Eqs. (A.1)–(A.3), (16), (17), (21), and (22) with two-term Taylor series yields

$$d_{m0}=1,\quad d_{m1}=0,\quad d_{m2}=\frac{(M+1)Gz}{8\kappa^2}\lambda_m,$$
$$d_{m3}=0,\ldots,\quad d_{mn}=\frac{(M+1)Gz}{2\kappa^2[n(n-1)+n]}\lambda_m\left(d_{mn-2}-\frac{d_{mn-4}}{\kappa^2}\right), \tag{A.4}$$

$$e_{m0}=1,\quad e_{m1}=0,\quad e_{m2}=-\frac{1}{8}\frac{(M+1)Gz\lambda_m}{W_1(1-\kappa^2)}\left(1-\frac{3W_2}{2}\right),$$
$$e_{m3}=-\frac{1}{9}\frac{(M+1)Gz}{W_1(1-\kappa^2)}\lambda_m W_2,\ldots,$$
$$e_{mn}=-\frac{(M+1)Gz\cdot\lambda_m}{2W_1(1-\kappa^2)[n(n-1)+n-1]} \times\left[\left(1-\frac{3W_2}{2}\right)e_{mn-2}+2W_2e_{mn-3}-\left(1+\frac{W_2}{2}\right)e_{mn-4}\right]. \tag{A.5}$$

References

[1] R.K. Shah, A.L. London, in: Laminar Flow Forced Convection in Ducts, Academic Press, New York, 1978, pp. 196–207.
[2] V.-D. Dang, M. Steinberg, Convective diffusion with homogeneous and heterogeneous reaction in a tube, J. Phys. Chem. 84 (1980) 214–219.
[3] T.L. Perelman, On conjugated problems of heat transfer, Int. J. Heat Mass Transfer 3 (1961) 293–303.
[4] D. Murkerjee, E.J. Davis, Direct-contact heat transfer immiscible fluid layers in laminar flow, AIChE J. 18 (1972) 94–101.
[5] S.S. Kim, D.O. Cooney, Improved theory for hollow-fiber enzyme reactor, Chem. Eng. Sci. 31 (1976) 289–294.
[6] E.J. Davis, S. Venkatesh, The solution of conjugated multiphase heat and mass transfer problems, Chem. Eng. Sci. 34 (1979) 775–787.
[7] E. Papoutsakis, D. Ramkrishna, Conjugated Graetz problems. I: general formalism and a class of solid–fluid problems, Chem. Eng. Sci. 36 (1981) 1381–1390.
[8] E. Papoutsakis, D. Ramkrishna, Conjugated Graetz problems. II: fluid–fluid problems, Chem. Eng. Sci. 36 (1981) 1393–1399.
[9] X. Yin, H.H. Bau, The conjugated Graetz problem with axial conduction, Trans. ASME 118 (1996) 482–485.
[10] J. Korpijarvi, P. Oinas, J. Reunanen, Hydrodynamics and mass transfer in airlift reactor, Chem. Eng. Sci. 54 (1998) 2255–2262.
[11] E. Santacesaria, M. Di Serio, P. Iengo, Mass transfer and kinetics in ethoxylation spray tower loop reactors, Chem. Eng. Sci. 54 (1999) 1499–1504.
[12] E. Garcia-Calvo, A. Rodriguez, A. Prados, J. Klein, Fluid dynamic model for three-phase airlift reactors, Chem. Eng. Sci. 54 (1998) 2359–2370.
[13] M. Atenas, M. Clark, V. Lazarova, Holdup and liquid circulation velocity in a rectangular air-lift bioreactor, Ind. Eng. Chem. Res. 38 (1999) 944–949.
[14] S. Goto, P.D. Gaspillo, Effect of static mixer on mass transfer in draft tube bubble column and in external loop column, Chem. Eng. Sci. 47 (1992) 3533–3539.

[15] K.I. Kikuchi, H. Takahashi, Y. Takeda, F. Sugawara, Hydrodynamic behavior of single particles in a draft-tube bubble column, Can. J. Chem. Eng. 77 (1999) 573–578.
[16] S.N. Singh, The determination of eigen-functions of a certain Sturm–Liouville equation and its application to problems of heat-transfer, Appl. Sci. Res. A 32 (1958) 237–250.
[17] G.M. Brown, Heat or mass transfer in a fluid in laminar flow in a circular or flat conduit, AIChE J. 6 (1960) 179–183.
[18] R.J. Nunge, W.N. Gill, An analytical study of laminar counterflow double-pipe heat exchangers, AIChE J. 12 (1966) 279–289.
[19] R.J. Nunge, E.W. Porta, W.N. Gill, Axial conduction in the fluid streams of multistream heat exchangers, Chem. Eng. Progr. Symp. Series 63 (1967) 80–91.
[20] S.W. Tsai, H.M. Yeh, A study of the separation efficiency in horizontal thermal diffusion columns with external refluxes, Can. J. Chem. Eng. 63 (1985) 406–411.
[21] H.M. Yeh, S.W. Tsai, C.S. Lin, A study of the separation efficiency in thermal diffusion columns with a vertical permeable barrier, AIChE J. 32 (1986) 971–980.
[22] H.M. Yeh, S.W. Tsai, T.W. Chang, A study of the Graetz problem in concentric-tube continuous-contact counter-current separation processes with recycles at both ends, Sep. Sci. Technol. 21 (1986) 403–419.
[23] M.A. Ebadian, H.Y. Zhang, An exact solution of extended Graetz problem with axial heat conduction, Int. J. Heat Mass Transfer 32 (1989) 1709–1717.
[24] C.D. Ho, H.M. Yeh, W.S. Sheu, An analytical study of heat and mass transfer through a parallel-plate channel with recycle, Int. J. Heat Mass Transfer 41 (1998) 2589–2599.